

Effect of Valine and Glycine as Environmentally Safe Inhibitors on Dissolution of α -Aluminum Bronze in Sulfide Polluted Saltwater: Electrochemical and Stress Corrosion Cracking Study

Lobna A. Khorshed¹, Ahmed Abdel Nazeer^{1,2}, Fadhel A. Azeez², E.A. Ashour¹

1. National Research Centre, Electrochemistry and Corrosion Lab., Dokki, Cairo, Egypt 12622.

2. Chemical Engineering Department, Kuwait University, P.O. Box 5969, Safat 13060, Kuwait.

Received 11 Jan 2017,
Revised 03 Jun 2017,
Accepted 09 Jun 2017

Keywords

- ✓ α -Al bronze alloy;
- ✓ Valine and Glycine;
- ✓ Corrosion;
- ✓ Sulfide;
- ✓ SEM and EDX.

Ahmed Abdel Nazeer
anazeer_nrc@yahoo.com
+96599515318

Abstract

Herein, the inhibiting effect of valine and glycine to suppress the dissolution of α -Aluminum bronze (Cu7Al) alloy, in chloride electrolyte with and without sulfide ions was studied. Different techniques were used such as potentiodynamic polarization, electrochemical impedance spectroscopy (EIS), electrochemical frequency modulation (EFM) and stress corrosion cracking (SCC) using the constant slow strain rate technique (SSRT). The surface morphology was examined using SEM and EDX to evaluate the effect of studied inhibitors. The protection of α -Aluminum bronze is attributed to the formation of protective film of the amino acids on the alloy surface which decreases in presence of sulfide ions due to the incorporation of sulfur in the protective film and the corrosion increases. SEM and EDX results confirmed the presence of protective layer on the alloy surface in presence of the studied amino acids. The presence of valine and glycine changes the failure mode from brittle transgranular cracking to ductile failure. The data obtained from potentiodynamic polarization, EIS and EFM are in good agreement with SSRT results.

1. Introduction

Copper-base alloys are important constructional materials for many industrial applications because of their excellent thermal, electrical, and mechanical properties [1, 2]. The stability of these alloys in the different environments is attributed to the formation of protective and adherent films of corrosion products namely (Cu₂O), (Cu₂(OH)₃Cl), (CuO) and other oxides of the alloying elements [3, 4]. One of the most important copper-base alloys is α -Aluminum bronze (Cu7Al) with Al content less than 14%, which is extensively used in impellers, turbines, valves, and different marine applications due to its excellent corrosion and erosion resistance by formation of a protective film of Al₂O₃ [5, 6]. In spite of the remarkable resistance of this alloy towards several chemicals and atmospheres it still susceptible to corrosion in aggressive media. Many researchers studied the aggressive effects of common pollutants on the corrosion behavior of α -Al bronze and its susceptibility to stress corrosion cracking such as chloride [7], nitrite [5], sulfide [8] and desalination environment [9].

The presence of sulfide ions in the seawater is an important factor that accelerates the corrosion process of α -Al bronze alloy. These ions modify the character of the corrosion product film. The presence of sulfide ions is more dangerous when the corroding medium contains dissolved oxygen [10]. Lee and Hack reported that corrosion rate of Cu-base alloys increases by a factor of 10 to 30 when seawater contains sulfur compounds as impurities [11]. Protection of copper and its alloys against corrosion in many industries was performed using different organic corrosion inhibitors due to the presence of heteroatoms (S, N and P) in the molecular structure of the inhibitors [12]. Azoles are common corrosion inhibitors used for copper and its alloys in industry and their

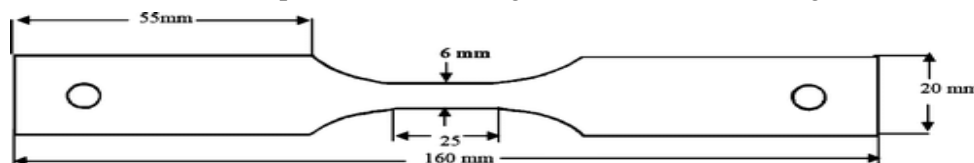
corrosion inhibition effect is related to the formation of an insoluble film on the electrode surface which suppresses the metal oxidation [13]. Toxicity of the azoles and its expensive price when needed in pure analytical grades limit their use. Therefore, it is important to investigate cheap, non-toxic and environmentally friendly corrosion inhibitors. Recently, different natural compounds containing of different hetero atoms have been reported as effective corrosion inhibitors for different metals and alloys due to their important properties such as; environmentally safe, cheap, and their availability [14-20].

Amino acids were successfully used as potential and non-toxic corrosion inhibitors for various metals and alloys in different aggressive environments [21-28]. The choice of amino acids is based on the presence of electron cloud of the heteroatom (S, N and O) and also these compounds are relatively cheap, environmentally safe and produce easily with purities greater than 99%.

Abdel Nazeer et al., [8] reported the inhibition of α -Al bronze in clean and sulfide-polluted salt water using 5-methyl 1-H benzotriazole but still there is lack of reports on the corrosion inhibition of α -Al bronze in sulfide polluted media using environmentally friendly inhibitors. The current work aims to study the effect of valine and glycine as environmentally friendly inhibitors to protect α -Al bronze from dissolution in sulfide polluted saltwater. Different electrochemical measurements such as potentiodynamic polarization, EIS and EFM techniques were studied. Also the susceptibility of α -Al bronze to SCC and its protection was investigated.

2. Experimental details

The working electrode was prepared from a commercial α -Al bronze alloy with composition of 7.0% Al, 0.01% Ni, 0.04 Fe, 0.04 Si, 0.006 Mg and the rest copper. The measurements of polarization curves, EFM and EIS are carried out in a three electrode cell in simulated seawater media. A saturated calomel electrode (SCE) as a reference electrode, a platinum foil as a counter electrode, and alloy specimen as a working electrode was used. Polarization measurements were performed using a PS6 Meinsperger Potentiostat/Galvanostat (Germany) at scan rate of 1 mV s^{-1} . EFM and EIS measurements were carried out with a Potentiostat/Galvanostat (Gamry PCI 300/4). For EFM measurements, a potential perturbation signal with amplitude of 10 mV with two sine waves of 2 and 5 Hz was applied. The intermodulation spectra containing current responses were assigned for harmonical and intermodulation current peaks. The frequency spectrum of the current response was used to calculate the causality factor which is very important to validate the data if these two factors CF2 and CF3 have values about 2.0 and 3.0, respectively. The larger peaks were used to calculate the corrosion current density (i_{corr}), the Tafel constants (β_c and β_a) and the causality factors CF2 and CF3. The EIS experiments were performed at open circuit potential with amplitude of 10 mV in the frequency range between 100 kHz and 10 mHz. For SCC experiments the optimum strain rate for testing the SCC susceptibility depends largely on the metal environment system or the crack propagation rate (CPR). In this study the constant strain rate tensile tests were carried out by applying a constant strain rate of $5.53 \times 10^{-6} \text{ sec}^{-1}$ which was found to be the optimum value of SCC of α -Al bronze in similar solution [29]. The test cell was in the form of a glass cylinder (120 mm in height and 80 mm in diameter). It was closed at the top and bottom by rubber stopper through which the ends of the specimens protruded. The lower end of the specimen was sealed to the lower rubber stopper by paraffin wax to prevent leakage of the solution. The tensile test specimens were designed to have the following dimensions:



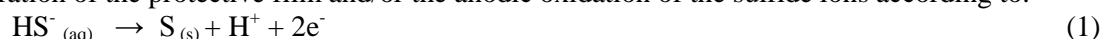
Before conducting the tests, the specimens were polished with 600, 800 and 1200 SiC grit papers, degreased with acetone, rinsed with distilled water. The studied surfaces were examined using a Philips Energy Dispersive X-ray diffractometer (pw-1390) with a Cu-tube ($\text{CuK}\alpha 1$, $\lambda = 1.54051 \text{ \AA}$) and also a scanning electron microscope model LEO SUPRA 50VP, Germany.

3. Results and Discussion

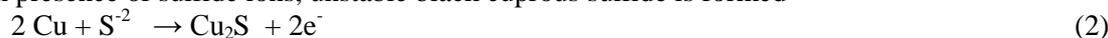
3.1. Potentiodynamic polarization measurements

The potentiodynamic polarization curves of Cu7Al alloy in aerated chloride solution containing 100ppm sulfide in absence and presence of different concentrations of valine are presented in Figure 1A. Similar curves in presence of glycine were also recorded as shown in Figure 1B. The measurements were carried out after 30 min until reaching a steady state potential at a scan rate of 1.00 mVs⁻¹ within the potential range from -1.0 to 0V vs. saturated calomel electrode. Values of corrosion potential (E_{corr}) and corrosion current density (i_{corr}) obtained by extrapolation of the cathodic (β_c) and anodic (β_a) Tafel slopes are given in Table 1. From the obtained results it is obvious that in presence of 100ppm sulfide ions the corrosion current density is relatively high in the cathodic part due to hydrogen evolution reaction. Also the corrosion potential was observed at highly negative corrosion potential (-0.88V).

It is well known that copper alloys exhibits high corrosion resistance in chloride media due to formation the soluble copper chloride complex CuCl₂⁻ and Cu₂O [30, 31]. In case of aluminum bronze, the presence of an inner adherent layer of Al₂O₃ and an outer layer of Cu₂O are responsible for its corrosion resistance [32]. In presence of sulfide, the corrosion currents increased noticeably and this increase can be attributed to the deterioration of the protective film and/or the anodic oxidation of the sulfide ions according to:



Also, in presence of sulfide ions, unstable black cuprous sulfide is formed



The formation of Cu₂S and CuS which act as corrosion promoters prevent the formation of the protective layer of Cu₂O [33].

In the presence of valine and glycine as corrosion inhibitors, the anodic and cathodic polarization curves were markedly shifted toward more noble potentials compared to that in absence of the inhibitors. Also, the shift in free corrosion potential in the noble direction increases by increasing the inhibitor concentration. Moreover, the corrosion current density decreases by increasing the inhibitors concentration as shown in Table 1.

Table 1. Electrochemical parameters obtained from potentiodynamic polarization measurements of α Al-bronze alloy in 3.5%NaCl + 100ppm S²⁻ (blank) in the absence and presence of various concentrations of glycine and valine.

Conc., ppm	i _{corr.} , mA	-E _{corr.} , mV	-β _c , mV dec. ⁻¹	β _a , mV dec. ⁻¹	θ	I%	Corrosion rate (CR) mm/year
blank	0.0067	880	18.75	23.4468	-	-	0.077
blank + 20ppm glycine	0.0012	820	39.71	16.8009	0.819	81.9	0.014
blank + 40ppm glycine	0.0011	676	53.76	26.8895	0.834	83.4	0.013
blank + 60ppm glycine	0.0010	641	31.04	18.7775	0.853	85.3	0.011
blank + 80ppm glycine	0.0008	623	27.25	15.7650	0.879	87.9	0.010
blank + 20ppm valine	0.0026	798	16.36	18.7032	0.616	61.6	0.030
blank + 40ppm valine	0.0017	688	28.73	48.4878	0.744	74.4	0.020
blank + 60ppm valine	0.0014	650	17.21	17.1231	0.787	78.7	0.017
blank + 80ppm valine	0.0007	585	20.21	21.6573	0.898	89.8	0.008

The lowest corrosion current obtained in presence of 80ppm valine (0.68 μA cm⁻²) compared to (6.67 μA cm⁻²) in the sulfide polluted salt water in absence of inhibitor. The inhibition efficiency of the studied inhibitors to control the Aluminum bronze dissolution was calculated from polarization curves using the following equation [34]:

$$\text{I\%} = \frac{[i_{\text{corr}} - i_{\text{corr}}(\text{inh})]}{i_{\text{corr}}} \times 100 \quad (3)$$

where i_{corr} and i_{corr}(inh) are the corrosion current density in the absence and presence of the studied inhibitors, respectively.

Using equation 3 and from the data in Table 1 it is clear that the inhibition efficiency increases with increasing the inhibitor concentration. The maximum inhibition obtained for the studied inhibitors is 89.8% in presence of 80ppm valine and 87.9% in presence of 80ppm glycine. The results confirmed that the investigated inhibitors presented an inhibiting effect on both anodic dissolution of copper and cathodic hydrogen evolution reaction which recommended there using as effective environmentally friendly inhibitors for Aluminum bronze in the sulfide polluted media.

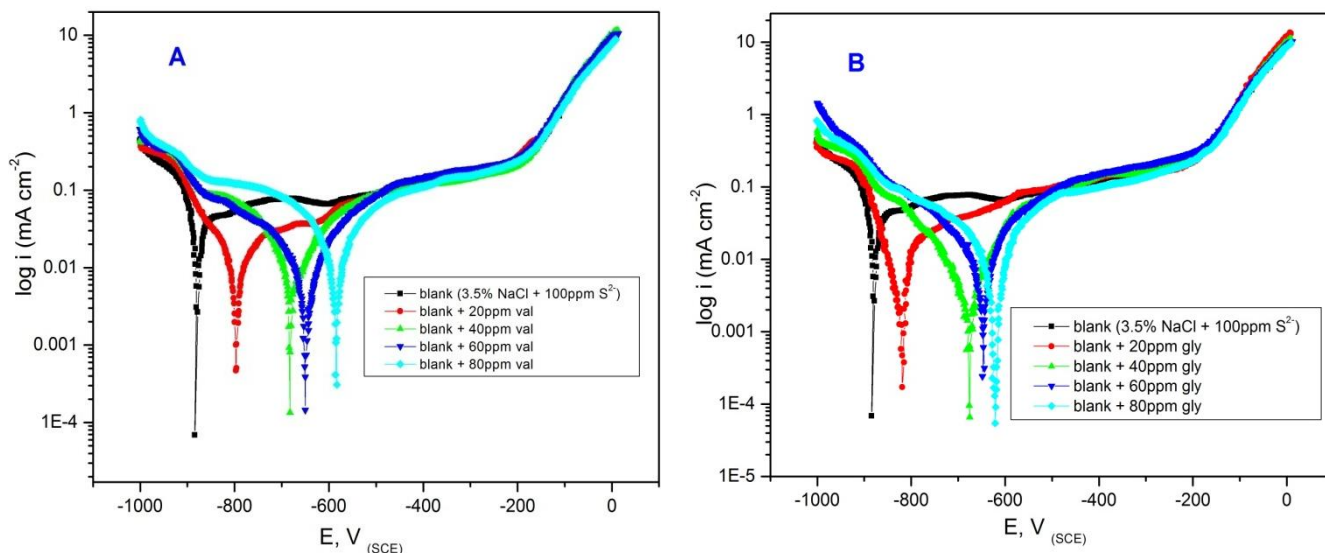


Figure 1. Polarization curves of α Al-bronze alloy in 3.5 % NaCl + 100ppm sulfide (blank) alone and with different concentrations of (A) Valine and (B) glycine

3.2. Electrochemical frequency modulation measurements (EFM)

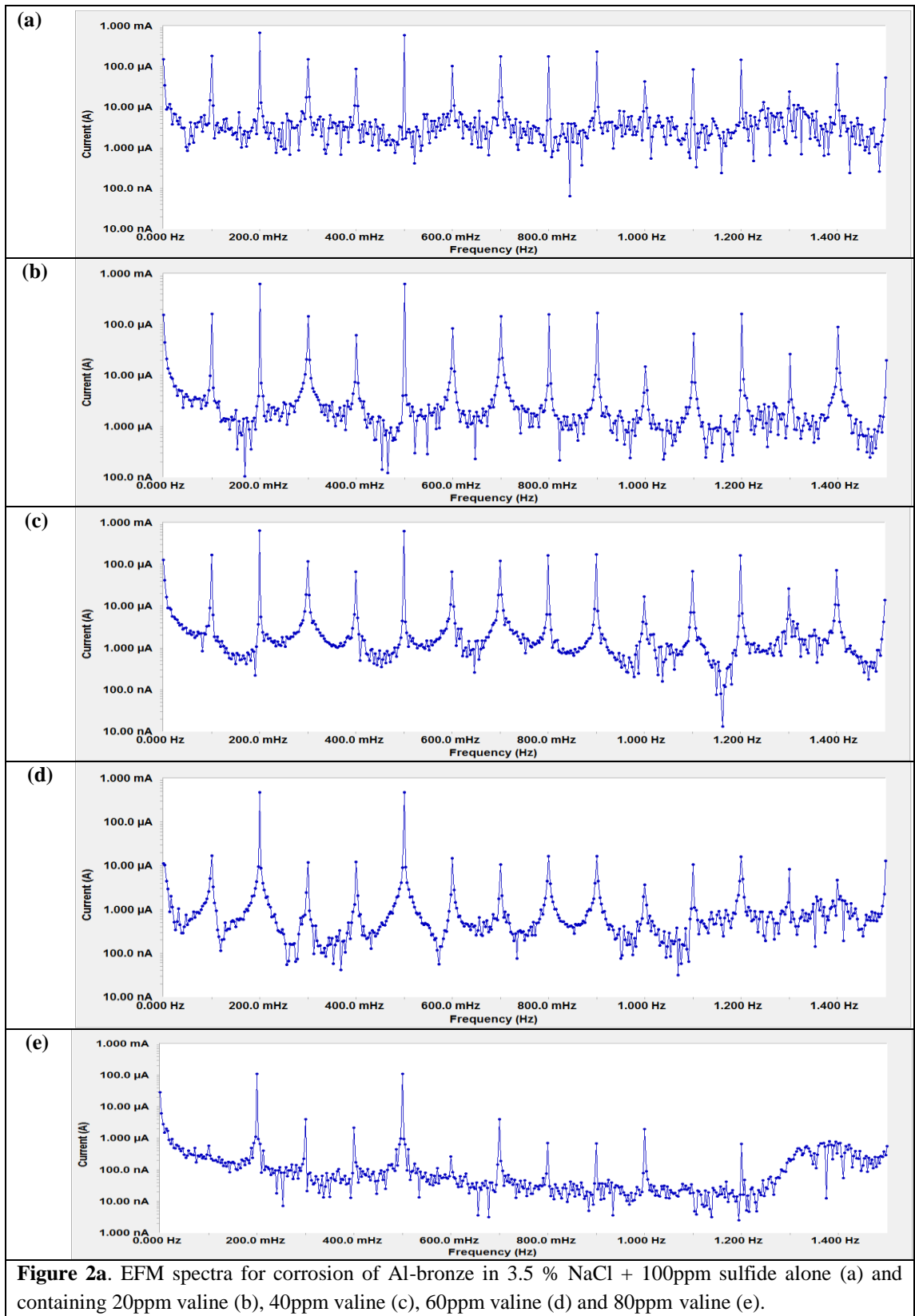
As a nondestructive corrosion measurement technique, EFM can be directly applied to give the corrosion current values without prior knowledge of Tafel constants. The EFM technique has been used to calculate the anodic and cathodic Tafel slopes as well as corrosion current densities for Al-bronze alloy in sulfide polluted salt water (3.5% NaCl + 100ppm S^{2-}) in the absence and presence of different concentrations of the studied amino acids (glycine and valine) as shown in Fig 2 (a, b). Each spectrum is a current response as a function of frequency. The different electrochemical parameters (corrosion current density (i_{corr}), the Tafel slopes (β_a and β_c) and the causality factors (CF-2 and CF-3)) were calculated from the largest peak in EFM spectrum and given in Table 2. From this Table, one can conclude that the corrosion current densities decrease by increasing the concentration of the studied amino acid.

Inhibition efficiency ($I_{EFM}\%$) depicted in Table 2 was calculated from the following equation:

$$I_{EFM} (\%) = [(i_{corr} - i_{corr(inh)}) / i_{corr}] \times 100 \quad (4)$$

Where i_{corr} and $i_{corr(inh)}$ are corrosion current densities in the absence and presence of the studied amino acids, respectively.

The inhibition efficiency increases by increasing the concentration of the studied amino acids, reached 73.1 % in presence of 80ppm of valine, and 56.2 in presence of 80ppm of glycine. Also the causality factors CF-2 and CF-3 are close to their theoretical values of 2 and 3, respectively indicating that the measured data are of high quality which confirms the validity of Tafel slopes and corrosion current densities according to EFM theory [35]. In conclusion, it is clear that using valine showed more pronounced inhibition efficiency than glycine. Moreover, the results showed good agreement of corrosion kinetic parameters obtained from EFM with those obtained from potentiodynamic polarization method.



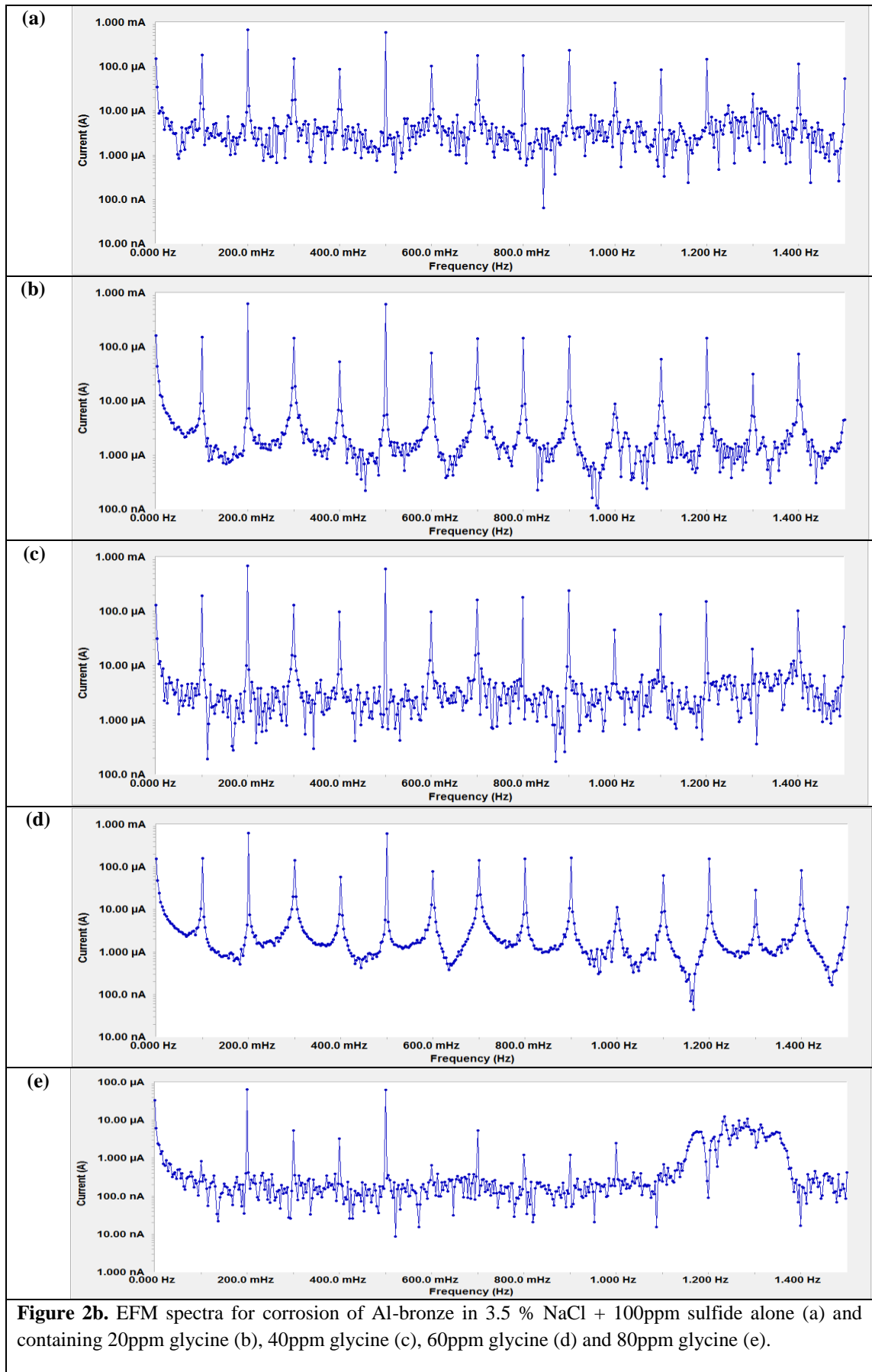


Figure 2b. EFM spectra for corrosion of Al-bronze in 3.5 % NaCl + 100ppm sulfide alone (a) and containing 20ppm glycine (b), 40ppm glycine (c), 60ppm glycine (d) and 80ppm glycine (e).

Table 2. Electrochemical parameters obtained by EFM technique for α Al-bronze in 3.5%NaCl + 100ppm S²⁻ (blank) in the absence and presence of various concentrations of glycine and valine.

Conc.	i_{corr} $\mu\text{A cm}^{-2}$	β_a , mV dec^{-1}	$-\beta_c$, mV dec^{-1}	CF-2	CF-3	θ	$I_{\text{EFM}}\%$
blank	19.8	104	197	1.94	3.04	-	-
blank + 20ppm glycine	17.22	92	167	2.02	2.92	0.130	13.0
blank + 40ppm glycine	13.68	81	158	1.96	2.97	0.309	30.9
blank + 60ppm glycine	10.79	65	143	1.92	2.89	0.455	45.5
blank + 80ppm glycine	8.66	59	127	1.91	2.84	0.562	56.2
blank + 20ppm valine	14.92	92	175	1.91	2.94	0.245	24.5
blank + 40ppm valine	10.76	78	158	1.96	2.99	0.457	45.7
blank + 60ppm valine	7.52	84	146	1.89	2.90	0.620	62.0
blank + 80ppm valine	5.32	70	138	1.92	2.87	0.731	73.1

3.3. Electrochemical impedance spectroscopy (EIS)

Electrochemical impedance spectroscopic measurements has found its valuable application in the field of corrosion due to the vital information that is extracted about the electrode surface, metal-electrolyte interface, analyzing the kinetic properties and determining the mechanism of interaction [36].

The corrosion behavior of Al-bronze alloy in 3.5% NaCl + 100 ppm S²⁻ in the absence and presence of different concentrations of glycine and valine was investigated by EIS method. Figure 3a, b shows the Nyquist plots with an applied frequency range from 100 kHz to 0.1 Hz at an applied dc potential of 0 V versus OCP. Depressed semicircles with their centers below the real axis were obtained from the Nyquist plots rather than the perfect semicircle expected from the EIS theory which can be attributed to the frequency dispersion effect due to electrode surface roughness and inhomogeneity. The heterogeneity of the electrode surface resulting from surface roughness, impurities, adsorption of inhibitors and formation of porous layers [37].

To give a more accurate fit for the results, a constant phase element (CPE) is substituted for the capacitive element.

The CPE impedance (Z_{CPE}) is obtained by:

$$Z_{\text{CPE}} = Y_0^{-1}(j \omega)^{-n} \quad (5)$$

where Y_0 and n are the admittance and exponent of CPE of the electrical double layer, respectively. Also, ω is the angular frequency ($\omega = 2\pi f$, where f is the AC frequency), and j here is the imaginary unit. For n value equal to 1, 0 and -1, CPE is reduced to the capacitor (C), resistance (R) and inductance (L), respectively. However, a value of $n = 0.5$ corresponds to Warburg impedance (W).

Determining the correction of the capacity to its real value is calculated using the following equation:

$$C_{\text{dl}} = Y_0 (\omega_{\text{max}})^{n-1} \quad (6)$$

where ω_{max} is the frequency at which the imaginary component of the impedance ($-Z_i$) is maximum.

An equivalent circuit was proposed to represent the corrosion of Al-bronze in sulfide polluted salt water in absence and presence of the studied inhibitors, as shown in Fig. 4a and Fig. 4b, respectively. R_s is the solution resistance, R_{ct} is the charge-transfer resistance, and C_{dl} is the double-layer capacitance. The equivalent circuit used in presence of the studied inhibitors contains two time constants, one in the high frequency region due to the fast charge transfer process of alloy dissolution (R_1C_1) and the other in the low impedance region (R_2C_2) due to the mass transport through the oxide film. The data obtained from the fitted spectrum are listed in Table 3.

The charge transfer resistance values increase noticeably in presence of the studied inhibitors in sulfide-polluted solution and which increases more with increasing the inhibitor concentration. This confirms the coverage and protection of the surface and results in a decrease in the rate of corrosion. On the other hand, it is well known

that the capacitance is inversely proportional to the thickness of the double layer and from Table 3; it is obvious that the double layer capacitance values, C_{dl} , decreases in presence of the studied inhibitors and decreases more with increasing the inhibitors concentration. The decrease in the C_{dl} , result from the local dielectric constant decrease and/or the thickness of the electrical double layer increase which suggests that these amino acids function by adsorption at the metal/solution interface [38].

The inhibition efficiency is calculated and presented in Table 3 as follow:

$$I_{EIS} \% = [(R_{ct(inh)} - R_{ct}) / R_{ct(inh)}] \times 100 \quad (7)$$

where $R_{ct(inh)}$ and R_{ct} are the charge-transfer resistances with and without the inhibitors, respectively. Form Table 3 it is clear that the inhibition efficiency increases with increasing the inhibitors concentration with maximum inhibition of 70.4 and 59.3 in presence of 80ppm of valine and glycine, respectively. The inhibition efficiency calculated from EIS results showed the same trend as those obtained from potentiodynamic polarization and EFM measurements. The difference of inhibition efficiency from the different methods may be attributed to the different surface status of the working electrode in the different measurements.

Table 3. Electrochemical kinetic parameters obtained by EIS technique for the corrosion of α Al-bronze in 3.5 % NaCl + 100ppm sulfide in presence of different concentrations of glycine and valine.

Conc.,	R_s $\Omega \text{ cm}^2$	C_1 $\mu\text{F cm}^{-2}$	n	R_1 $\Omega \text{ cm}^2$	C_2 $\mu\text{F cm}^{-2}$	n	R_2 $\Omega \text{ cm}^2$	$I_{EIS}\%$
blank	5.03	-	-	-	402	0.91	204	-
blank + 20ppm glycine	5.07	37	0.78	11	324	0.93	248	17.7
blank + 40ppm glycine	5.01	32	0.80	27	296	0.95	334	38.9
blank + 60ppm glycine	5.18	26	0.83	49	271	0.89	446	54.3
blank + 80ppm glycine	5.22	19	0.89	68	235	0.92	501	59.3
blank + 20ppm valine	5.09	24	0.81	44	306	0.93	294	30.6
blank + 40ppm valine	5.17	18	0.85	69	267	0.88	421	51.5
blank + 60ppm valine	5.22	14	0.86	82	234	0.85	576	64.6
blank + 80ppm valine	5.11	11	0.92	103	201	0.92	689	70.4

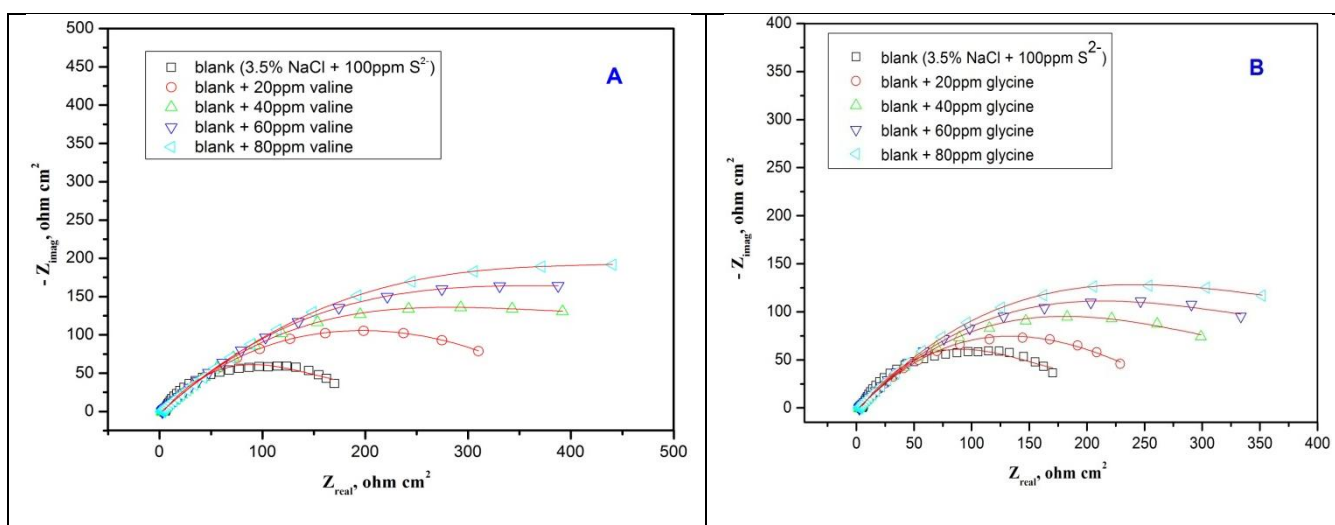


Figure 3. Nyquist plots recorded for α Al-bronze in 3.5 % NaCl + 100ppm S^{2-} with different concentrations of (A) valine and (B) glycine.

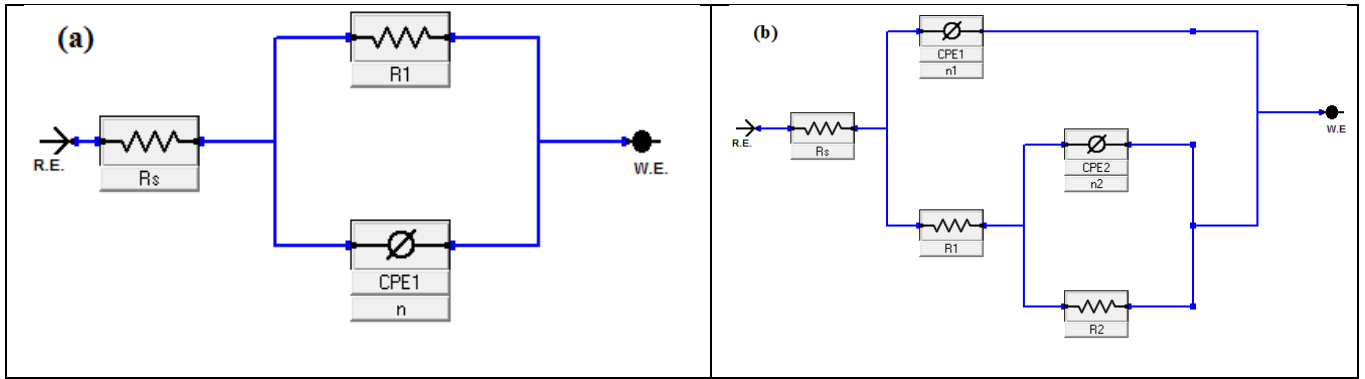


Figure 4. Equivalent circuit model used to fit the impedance spectra in absence (a) and presence (b) of the studied inhibitors.

3.4. SEM/EDX surface examination

The surface morphology of α Al-bronze alloy was investigated in aerated chloride solution containing 100ppm sulfide in absence and presence of different concentrations of valine and glycine after 24h of immersion. Figure 5a shows SEM micrograph in the chloride containing sulfide solution which reveals the dangerous growth of localized attack on the alloy surface resulted from the interference of sulfide ions with the normal growth of the protective oxide film of Cu_2O showing this deleterious effect.

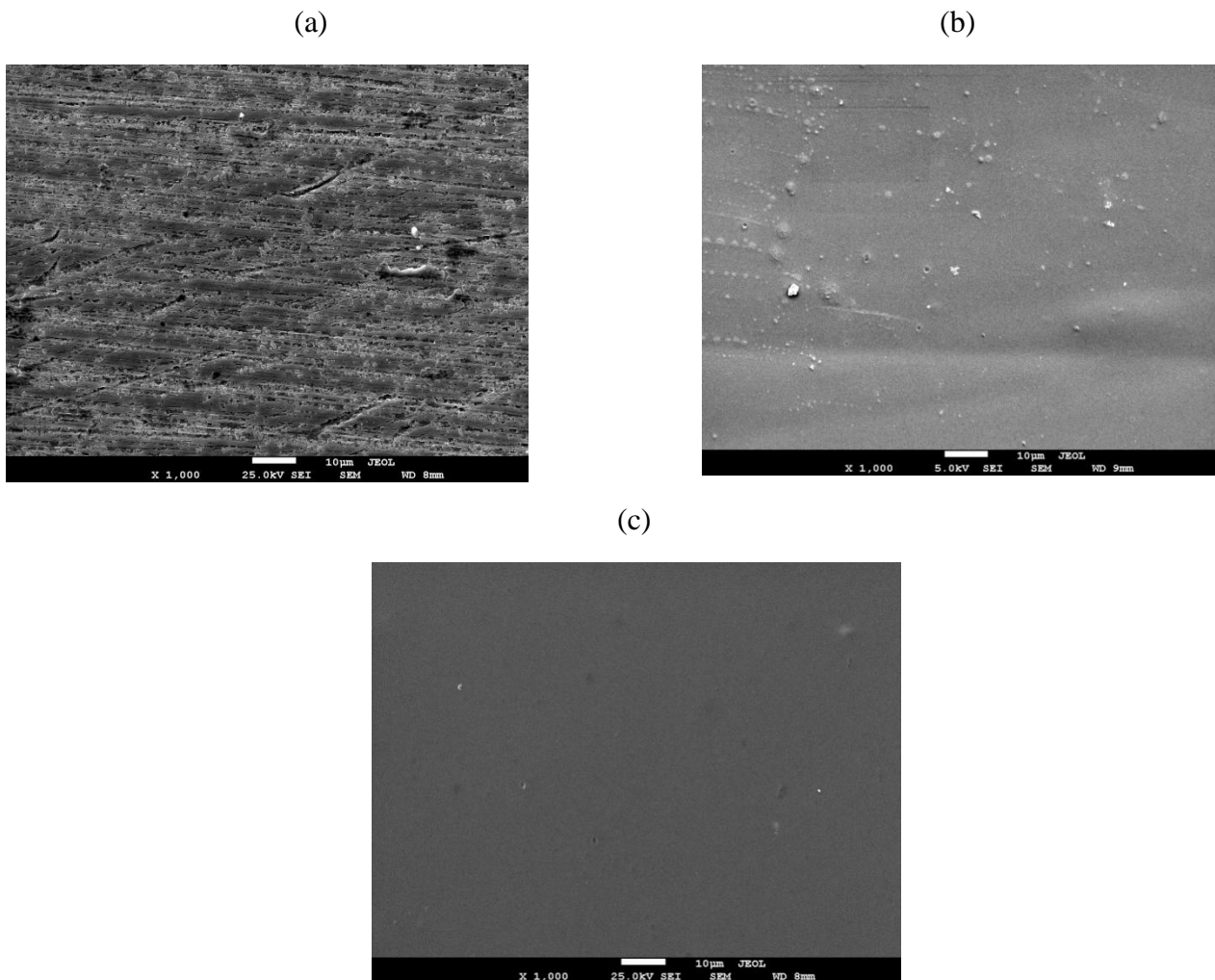


Figure 5. SEM micrograph of α Al-bronze alloy after immersion for 24 hour in 3.5%NaCl +100ppm S^{2-} (blank) alone (a) and with 80ppm of glycine (b) and with 80ppm of valine (c).

The effect of addition of 80ppm of the studied inhibitors on the surface morphology of the bronze alloy was also studied (Fig. 5b, c). A marked inhibiting effect is shown in presence of the studied inhibitors by protecting the active sites on the alloy surface.

The energy dispersive X-ray spectroscopy (EDX) was used to characterize the corrosion products and it is clear the existence of C and N peaks in presence of valine and glycine which suggest the adsorption of these inhibitors on the electrode surface (Fig. 6). The percentage of Cu in presence of sulfide is low due to the aggressive effect of sulfide and formation of different compounds of copper chloride and sulfide. In presence of the studied inhibitors higher concentration of copper was obtained confirming the ability of these inhibitors to suppress the sulfide attack.

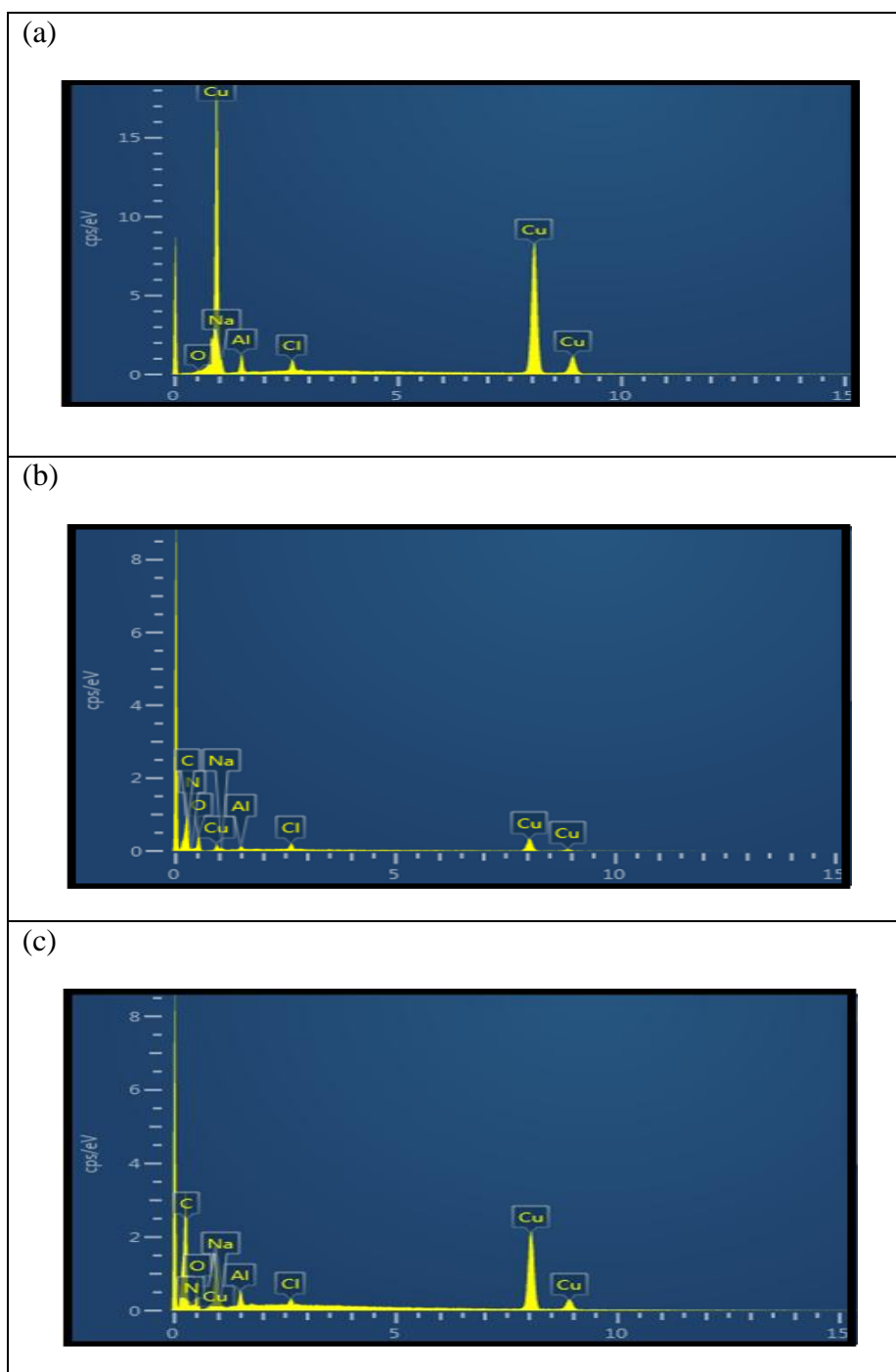


Figure 6. EDX spectra of α Al-bronze alloy after immersion for 24 hour in 3.5%NaCl + 100ppmS²⁻ (blank) alone (a) and with 80ppm of glycine (b) and valine(c).

3.5. Stress corrosion cracking (SCC) and failure mode measurements:

The use of glycine and valine as an environmentally friendly corrosion inhibitor was investigated for the SCC of Al-bronze under the aggressive media containing 100ppm of sulfide ions. Stress-strain curves were recorded in 3.5% NaCl + 100ppm S in the absence and presence of 500ppm of glycine and valine at strain rate of $5.53 \times 10^{-6} \text{ s}^{-1}$ under open circuit conditions as shown in Figure 7. Measurements were also performed in air for comparison. The maximum stress (σ), stress ratio (τ), time to failure (t_f), time to failure ratio (r), susceptibility to SCC (S) and mode of failure for samples tested under the various conditions were measured and summarized in Table 4.

Table 4. Stress corrosion cracking (SCC) parameters of α Al-bronze alloy in 3.5 % NaCl + 100ppm S^{2-} (blank) alone and with 500ppm of glycine and valine at strain rate of $5.53 \times 10^{-6} \text{ s}^{-1}$.

Medium	σ	T_f (min.)	r	τ	S	Failure mode
air	57.61	437	-	-	-	ductile
blank (3.5% NaCl +100 ppm S^{2-})	49.60	405	0.86	0.93	0.09	brittle
blank + 500ppm glycine	52.23	414	0.92	0.95	0.06	ductile
blank + 500ppm valine	54.64	431	0.95	0.99	0.02	ductile

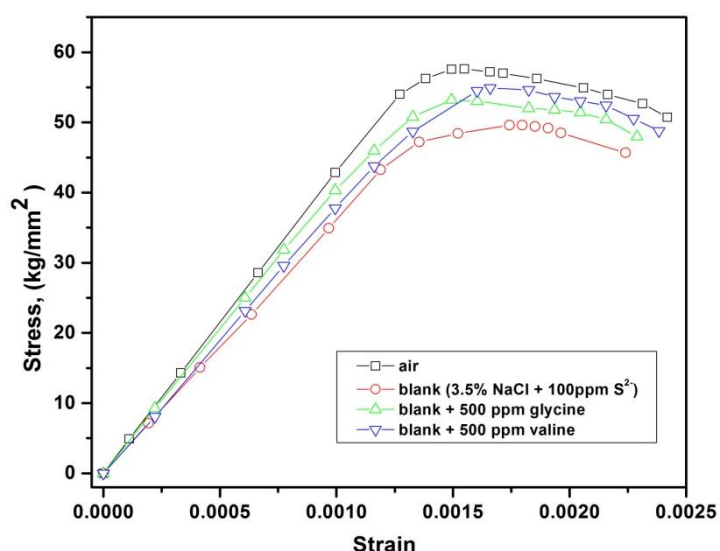


Figure 7. Stress-strain curves of α Al-bronze in air and in 3.5 % NaCl + 100ppm S^{2-} (blank) in presence of 500ppm of glycine and valine at strain rate $5.53 \times 10^{-6} \text{ s}^{-1}$.

The obtained curves characterized by an increase in strain with stress increasing till reaching the yield stress point, followed by a slight deviation from linearity and a gradual increase in the form of a plateau until reaching a maximum, then the strain begins to decline to reach the point of failure.

The maximum stress ratio is obtained using [39, 40]:

$$r = \frac{\sigma_{\max}(\text{sol})}{\sigma_{\max}(\text{air})} \quad (8)$$

Also the time to failure ratio is obtained using:

$$\tau = \frac{t_f(\text{sol})}{t_f(\text{air})} \quad (9)$$

Both r and τ were used to express the SCC susceptibility (S) given by:

$$S = [(1-r)(1-\tau)]^{1/2} \quad (10)$$

The presence of sulfide ion decreases the maximum stress and increases SCC of α -Al bronze alloy by the sulfide adsorption on copper surface which enhances the anodic copper dissolution reaction. It is clear that the addition of 500ppm of glycine and valine increases the ultimate stress and decreased the susceptibility (S) of the alloy to SCC from 0.09 in case of blank to 0.06 and 0.02 in presence of glycine and valine, respectively.

The SEM micrographs of α -Al-bronze samples subjected to SCC in 3.5% NaCl + 100 ppm S^{2-} alone and with 500ppm glycine and valine was shown in Fig. 8. It is clear that the fracture mode of failure in presence of sulfide is brittle transgranular as shown in Fig. 8a in which cleavage-like features was observed. The addition of 500 ppm of the studied amino acids to the aggressive media, changes the mode of failure from brittle transgranular to ductile one which is the same as in air confirming the inhibitive effect of the studied inhibitors for the SCC of α -Al bronze alloy due to their adsorption on the bronze surface and suppressing the anodic dissolution of the alloy.

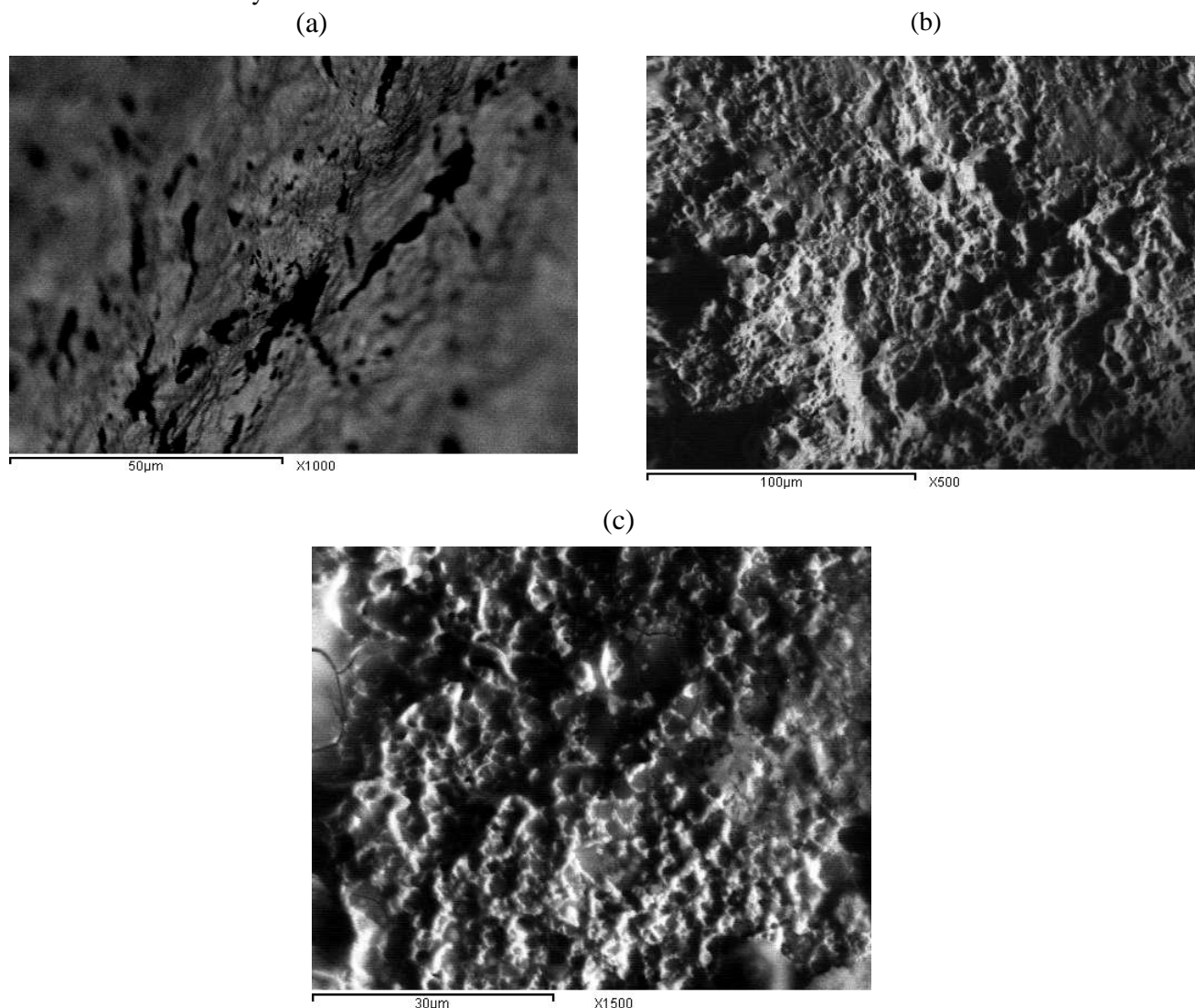


Figure 8. SEM fractograph of α Al-bronze in 3.5% NaCl + 100 ppm S^{2-} alone (a) and with 500ppm of glycine (b) and 500ppm of valine (c).

3.6. Mechanism of corrosion inhibition

In chloride solutions, it is well known that dissolution of copper base alloys occurs which leads to the formation of the insoluble $CuCl$ that transforms to $CuCl_2$ which is soluble copper chloride complex. The higher concentration of $CuCl_2$ at the alloy surface that leads to the formation of a Cu_2O layer [8]. This insight is in line

with results reported by Neodo et al. [41] confirming that the formation of cuprite (Cu_2O) during the copper oxidation in a chloride solution, at pH 6.2. Moreover, in case of α -aluminum bronze, an inner and adherent layer of Al_2O_3 was formed which explains the improved corrosion resistance of Cu-Al alloys. The corrosion-resisting properties of α -Al bronze are largely from the formation of stable surface film (Al_2O_3) on the metal.

Al_2O_3 as an inner adherent layer, acting as a barrier for ionic transport across the corrosion product and Cu_2O as an outer layer on Al bronze surfaces in sodium chloride solutions were confirmed by X-ray diffraction and Auger electron spectroscopy (AES) techniques [42].



The presence of aluminium oxide (Al_2O_3) often has been postulated to explain the improved corrosion resistance of Cu-Al alloys as compared to pure copper the ability of this oxide to heal rapidly in the work environment is the important criterion for application. In the presence of sulfide ions, unstable black cuprous sulfide is formed (Cu_2S) which affects the formation of the protective layer of the metals oxides (Cu_2O and Al_2O_3). Using valine and glycine as inhibitors lead to decreasing the dissolution of α -Aluminum bronze the alloy and hence increasing its inhibition where these amino acids contain two polar groups (amino group and carboxyl group) which can coordinate with the alloy surface through nitrogen atom and oxygen atom. The inhibition of corrosion by these amino acids is attributed to their adsorption of on the alloy surface. The protection of α -Aluminum bronze in presence of the studied amino acids is attributed to the formation of protective film of these inhibitors on the alloy surface which decreases in presence of sulfide ions due to the incorporation of sulfur in the protective film and the corrosion increases.

Conclusion

α -Al bronze alloy suffers from dissolution of copper and aluminum in the chloride containing-sulfide solution due to damaging the protective thin oxide film of copper oxide and formation of copper sulfide products. The studied amino acids (glycine and valine) protect the surface of Al-bronze alloy efficiently when subjected to sulfide-polluted chloride solution. The maximum protection efficiency was 89.81% obtained using 80ppm valine in the studied media using potentiodynamic polarization. The results obtained from polarization, EFM and EIS are in good agreement with SCC measurements. The presence of valine and glycine changes the mode of fracture from brittle transgranular cracking to ductile failure. SEM images showed a relative protection to the surface which confirmed using EDX showing carbon and nitrogen in the surface structure in case of exposure to sulfide in presence of the inhibitor.

References

1. Singh R.N., Verma N. and Singh W.R., *Corrosion*, 45 (1989) 222.
2. Syrett B.C., Wing S.S., *Corrosion*, 36 (1980) 73.
3. North R.F., Pryor M.I., *Corros. Sci.*, 10 (1970) 297.
4. Abdel Nazeer A., Allam N.K., Fouda A.S., Ashour E.A., *Mater. Chem. Phys.*, 136 (2012) 1.
5. Allam N.K., Abdel Nazeer A., Youssef G.I., Ashour E.A., *Corrosion*, 69 (2013) 77.
6. Ahmed Z., *Br. Corros. J.*, 11 (1976) 149.
7. Ateya B.G., Ashour E.A., and Sayed S.M., Stress Corrosion Behavior of α - Aluminum Bronze in Saline Water, *Corrosion*, 50 (1994) 20.
8. Abdel Nazeer A., Ashour E.A., Allam N.K., *Mater. Chem. Phys.*, 144 (2014) 55.
9. Thompson D.H., *Mater. Res. Std.*, 1 (1961) 108.
10. Syrett B.C., Macdonald D.D., Wing S.S., *Corrosion*, 35 (1979) 409.
11. Lee T.S., Hack H.P., Tipton D.G., Proceedings of the 5th International Congress on Marine corrosion and Fouling, (1980).
12. Allam N.K., *Appl. Surf. Sci.*, 253 (2007) 4570.
13. Ye X.R., Xin X.Q., Zhu J.J., Xue Z.L., *Appl. Surf. Sci.*, 135 (1998) 307.
14. Abdel Nazeer A., Shalabi K., Fouda A.S., *Res. Chem. Intermed.* 41 (2015) 4833.
15. Rahal C., Masmoudi M., Abdelhedi R., Sabot R., Jeannin M., Bouaziz M., Refait P., *J. Mol. Liq.* 215 (2016) 47.

16. Njoku D.I., Ukaga I., Ikenna O.B., oguzie E.E., oguzie K.L., Ibisi N., *J. Mol. Liq.* 219 (2016) 417.
17. Khadraoui A., Khelifa A., Hachama K., Mehdaoui R., *J. Mol. Liq.* 214 (2016) 293.
18. Shalabi K., Abdel Nazeer A., *Protection of Metals and Phys. Chem. Surf.* 51(5) (2015) 908.
19. Fouda A.S., Abdallah Y.M., Elawady G.Y., Ahmed R.M., *J. Mater. Environ. Sci.* 5 (6) (2015) 1519.
20. Barouni K., Kassale A., Albourine A., Jbara O., Hammouti B., Bazzi L., *J. Mater. Environ. Sci.* 5 (2) (2014) 456.
21. El-Rabiee M.M., Helal N.H., Abd El-Hafez Gh.M., Badawy W.A., *J. Alloys Compd.*, 459 (2008) 466.
22. Zhang D.Q., Cai Q.R., He X.M., Gao L.X., Kim G.S., *Mater. Chem. Phys.*, 114 (2009) 612.
23. Badawy W.A., Ismail K.M., Fathi A.M., *J. Appl. Electrochem.*, 35 (2005) 879.
24. Oguzie E.E., Li Y., Wang F.H., *Electrochim. Acta*, 53 (2007) 909.
25. Singh P., Bhrara K., Singh G., *Appl. Surf. Sci.*, 254 (2008) 5927.
26. Yadav, M., Gope, L. & Sarkar, T.K., *Res. Chem. Intermed.* 42 (2016) 2641.
27. Awad M.I., Saad A.F., Shaaban M.R., AL Jahdaly B.A., Hazazi O.A., *Int. J. Electrochem. Sci.*, 12 (2017) 1657.
28. Jia-jun Fu, Su-ning Li, Ying Wang, Lin-hua Cao, Lu-de Lu, *J. Mater. Sci.*, 45 (22) (2010) 6255.
29. Ashour E.A., Khorshed L.A., Youssef G.I., Zakria H.M., Khalifa T.A., *Materials Sciences and Applications*, 5 (2014) 10.
30. Metikos-Hukovic M., Babic R., Skugor I., Grubac Z., *Corros. Sci.*, 53 (2011) 347.
31. Barcia O.E., Mattos O.R., Pebere N., Tribollet B., *J. Electrochem. Soc.*, 140 (1993) 2825.
32. Ateya B.G., Ashour E.A. and Sayed S.M., *J. Electrochem. Soc.*, 141 (1994) 71.
33. Eiselstein L.E., Syrett B.C., Wang S.S., Caligiuri R.D., *Corros. Sci.*, 23 (1983) 223.
34. Babu B.R., Holze R., *Br. Corros. J.*, 35 (2000) 204.
35. Bentiss F., Bouanis M., Mernari B., Traisnel M., Vezin H., Lagrenee M., *Appl. Surf. Sci.*, 253 (2007) 3696.
36. Macdonald J.R., "Impedance Spectroscopy," John Wiley and Sons, New York, (1987).
37. Abdel Nazeer A., El-Abbasy H.M., Fouda A.S., *Res. Chem. Intermed.*, 39 (2013) 921.
38. Gamry Echem Analyst Manual, (2003).
39. Allam N.K., Abdel Nazeer A., Ashour E.A., *J. Solid State Electrochem.*, 16 (2012) 353.
40. Abdel Nazeer A., Allam N.K., Youssef G.I., Ashour E.A., *Ind. Eng. Chem. Res.*, 50 (2011) 8796.
41. Neodo S., Carugo D., Wharton J.A. and Stokes K.R., *J. Electroanal. Chem.*, 695 (2013) 38.
42. Schussler A., Exner H.E., *Corros. Sci.*, 34 (11) (1993) 1793.

(2017) ; <http://www.jmaterenvirosci.com>